Improving simultaneous and proportional control from EMG signals based on a Two-Stage Regression Structure

M. Shafieian and F. Nougarou

Dept. of Electrical and Computer Engineering, Université du Québec à Trois-Rivières, QC, Canada

Abstract— **A two-stage regression structure is proposed in this paper to improve simultaneous and proportional control based on electromyography (EMG) signals. Instead of considering the conventional approach with a regression model per degree of freedom (DoF), the proposed method applies a regression model per direction of each DoF: the 1st stage detects DoFs and then is used to select the direction models of the 2nd stage. By using linear regression on the data from one healthy experienced participant for 2 DoFs of his wrist, the proposed structure was evaluated offline with cross-evaluation and online with a real-time control of a cursor to hit some targets. The evaluation results showed a clear improvement of the proposed method in terms of accuracy, ability to reach the boundaries, reaction speed, accurate control and reactive control compared to the conventional approach. The potential of this structure also lies in the fact that it can use different regression methods, work for 3 DoFs and more and use the 1st stage knowledge to improve performance of the 2nd stage.**

Keywords— **EMG, simultaneous proportional control, regression, pattern recognition, offline and online evaluation.**

I. INTRODUCTION

Human machine interface (HMI) based on muscle activities provides an acceptable and natural approach for humans to interact in real-life applications with devices, such as prosthesis, clinical rehabilitation exoskeletons, and robotics [1]. In this type of HMI, the movements performed by a person are estimated from electromyography (EMG) signals and the estimates of these movements are used to control the given device in real time [2]. Among the different ways to detect muscle activity, surface EMG sensors are the most approach because they are easy to use and non-invasive [3].

In recent years, two main device control approaches based on EMG signals have been proposed: sequential control and simultaneous proportional control. Sequential control is a common strategy [4] which is based on classification methods in which predefined movements are associated with classes based on EMG signals, so that each class serves to control a device direction subsequently. This approach allows to detect a large number of movements from the signals with high accuracy: usually 10 classes with high accuracy of >95% [3, 5]. However, it is only possible to detect a finite number of predefined movements. This implies that sequential control can determine one movement at a time, which is robust but not intuitive. In contrast to sequential control, simultaneous and proportional control (SPC), mainly based on regression methods, aims to detect the degrees of freedom (DoF) of movements from EMG signals. Thus, by combining the detection of several DoFs, it is possible to detect non-predetermined movements (simultaneous) and to estimate their position at the same time, proportionally to the force exerted (proportional) [5-8]. This approach therefore has the potential to provide intuitive and accurate control from EMG.

Several approaches based on machine-learning regression methods was proposed in the literature to detect simultaneous and proportional forearm movements. Whether they are regression methods based on linear regression [8, 9], SVMs [10, 11], neural networks [11-13] or deep learning [14-16], the real-time detection accuracy is deteriorating for 3 DoFs and more, which is a crucial requirement for controlling a robotic arm or a prosthesis. It is why simultaneous and proportional control based on EMG signals for intuitively control of devices in real-time is not yet popularized despite of its potential [16].

The nature of EMG signals and the complexity of creating a model for each DoF, which involves the combination of several muscles, affect the possibility to correctly detect the two boundaries of a DoF in real-time. This problem of not being able to detect the boundaries of DoFs directly affects the accuracy and robustness of device control. The objective of this paper is to propose a structure based on two successive stages of regression in order to improve the detection accuracy and the ability to reach the boundaries of each DoF. To do this, the proposed method in this paper focuses on the detection of 2 DoFs of the wrist from the EMG signals of the forearm muscles. Instead of considering a regression model by DoF, this structure allows to consider a model for each direction. Thus, in the case of 2 DoFs, the 2 stages use 4 regression models (one for each direction) so that the 1st stage, based on the conventional approach, is used to select the direction, then the model of the 2nd stage is used. To demonstrate the usefulness of this structure, the models will be based on linear regression and an evaluation in simulation (offline) and in real-time (online) will be done with a single healthy participant.

The remainder of the paper is organized as follows. In section II, data acquisition as well as the proposed methods are described. Offline and online results are presented in section III. Finally, it is followed by conclusions in section IV.

II. MATERIALS AND METHODS

A. Data Acquisition

In this work, electromyographic (EMG) signals were recorded from forearm muscles using an EMG sensor with 8 electrodes or channels (MyoArmBand, Thalmic labs, Canada),

M. Shafieian is a PhD candidate in the Electrical and Computer Engineering Department, Université du Québec à Trois-Rivières, QC (corresponding author; e-mail: Mohammadali.Shafieian@uqtr.ca).

F. Nougarou is professor in the Electrical and Computer Engineering Department, Université du Québec à Trois-Rivières, QC (e-mail: Francois.Nougarou@uqtr.ca).

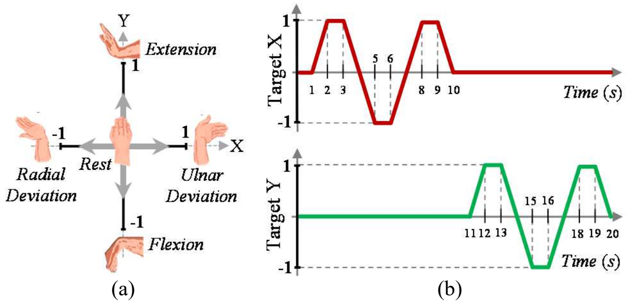

Figure1. (a) Movements of the wrist to perform X and Y DoFs, and (b) acquisition sequence of the X and Y displacements of the cursor.

placed around of the right forearm. The raw EMG signal, $e_i[n]$, of the i^{th} electrodes is a bipolar mode voltage; where i = 1, 2, …, N_c with N_c = 8 is the index of electrodes and n = 1, 2, …, N is the index of samples with N the number of samples and a sampling frequency of F_s= 200 Hz.

The present research has been realized using our home-made multi-system platform. This platform has been implemented, in MATLAB and Python, to record bio-signals by utilizing a user-interface guide so that some algorithms such as our proposed method can be developed, and their performances can be evaluated in offline. This platform also allows to test the algorithms' behaviors in real-time scenarios (to control a device or to play a game). Since the goal of this research was to propose a method for simultaneous and proportional control based on 2 DoFs of the wrist, the participant was asked to follow a cursor moving in the X and Y directions while his forearm EMG signals were recorded. As shown in Fig. 1 (a), the instructions given to the participant to perform this task are as follows: the X movements to the left and to the right correspond respectively to radial and ulnar deviation of the wrist, consequently Y movements to the top and to the bottom respectively to extension and flexion. In addition, the displacement boundaries are fixed to -1 and 1 for X and Y. Several acquisition sequences were recorded with a pause interval of 20 seconds between each sequence. Each acquisition sequence guided by a cursor on the screen consists of two repetitions for X and Y displacement presented in Fig. 1 (b). These X and Y displacements that the participant has to follow with his wrist are directly used to generate the target of the regression models. Once the EMG signals have been recorded through several acquisition sequences, the next phase therefore consists of segmentation, where the raw channel signals are windowed for feature extraction.

B. Features Extraction

The choice of features on the performance of movement detection based on EMG signals is very important. Concerning the detection of simultaneous and proportional movements, the features based on the characterization of the amplitude of the EMG signals in time-domain are privileged in the literature [17, 18]. For this reason, in this project, the following N_f= 3 features were extracted from the raw signals $e_i[n]$: the root mean square value (RMS), the mean average value (MAV) and the wavelength (WL) [19]. The choice of the size and the overlap between the windows are also very important because they constitute the stability and the reactivity trade-off of the estimates for the detection methods. We chose a window of 40 samples (200 ms) with an overlap of 35 samples which allows the detection method to provide an estimate for every 25 ms. It results two essential components from the windowing and features extraction: the features matrix $\mathbf{M}$ composed of $N_f \times N_c$= 24 rows and N_w columns, where N_w is the total number of windows and the target matrix $\mathbf{T}$ composed of 2 rows (the first one for X displacements and the second one for Y displacements) and N_w columns.

C. Two-Stage Regression

The proposed method is shown in Fig. 2 which consists of two stages to overcome the problems of unreached boundaries and to provide a good accuracy, compared to the conventional simultaneous and proportional detection for 2-DoFs wrist based on linear regression (LR). The idea for dealing with these challenges is not to use a model for every 2 DoF (X and Y), but to use 4 models for every 4 directions: X^- (to the left), X^+ (to the right), Y^- (down) and Y^+ (up). In this way, the models will be able to respond more specifically to each direction and improve the ability of reaching to the boundaries. In fact, the 1st stage which is based on a 2-DoFs regression method, will estimate the direction of wrist displacement and the 2nd stage will use the information from the 1st stage to select and use the direction-specific regression models. The learning and detection phases are described in the next sections.

D. Learning phase

The learning phase of the proposed simultaneous and proportional detection for 2 DoFs of the wrist is to create the models of the 2 stages as shown in Fig. 2 (a). The 1st stage estimates the X and Y displacements from the EMG signals with a linear regression method. For this purpose, two regression models, $\mathbf{w}_X$ and $\mathbf{w}_Y$, are calculated to estimate every 2 DoFs by using the ridge regression equations (1) and (2).

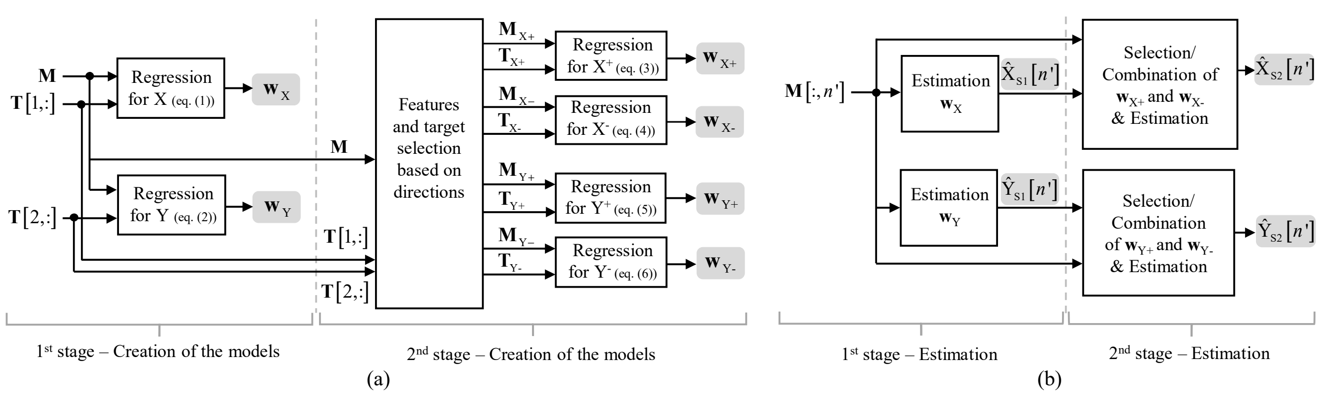

Figure 2. (a) Learning and (b) detection phases of the proposed simultaneous and proportional detection method based on EMG signals.

$$\mathbf{w}_{\mathrm{X}} = \left(\mathbf{M}\mathbf{M}^{\mathrm{T}} + \lambda\mathbf{I}\right)^{-1} \mathbf{M}\mathbf{T}[1,:]^{\mathrm{T}} \tag{1}$$

$$\mathbf{w}_{\mathrm{Y}} = \left(\mathbf{M}\mathbf{M}^{\mathrm{T}} + \lambda\mathbf{I}\right)^{-1} \mathbf{M}\mathbf{T}[2,:]^{\mathrm{T}} \tag{2}$$

where $\mathbf{M}$ is the features matrix, $\mathbf{T}$ is the target vector, λ= 0.1 and $\mathbf{I}$ is an identity matrix.

As mentioned above, the 2nd stage will estimate the 4 directions (X^-, X^+, Y^- and Y^+). It is therefore necessary to create a regression model for each direction. To do this, the vector $\mathbf{T}$ will be used to select the positions of the data corresponding to each direction, and then to define the features matrix and the target vector for each of them. Thus, we determine $\mathbf{M}_{X+}$, $\mathbf{T}_{X+}$, $\mathbf{M}_{X-}$, $\mathbf{T}_{X-}$, $\mathbf{M}_{Y+}$, $\mathbf{T}_{Y+}$ and $\mathbf{M}_{Y-}$, $\mathbf{T}_{Y-}$ respectively as the features matrices and the target vectors corresponding to the directions X^+, X^-, Y^+ and Y^-. For the regression models $\mathbf{w}_{X+}$, $\mathbf{w}_{X-}$, $\mathbf{w}_{Y+}$ and $\mathbf{w}_{Y-}$ we have:

$$\mathbf{w}_{\mathrm{X+}} = \left(\mathbf{M}_{\mathrm{X+}}\mathbf{M}_{\mathrm{X+}}^{\mathrm{T}} + \lambda\mathbf{I}\right)^{-1} \mathbf{M}_{\mathrm{X+}}\mathbf{T}_{\mathrm{X+}}^{\mathrm{T}} \tag{3}$$

$$\mathbf{w}_{\mathrm{X-}} = \left(\mathbf{M}_{\mathrm{X-}}\mathbf{M}_{\mathrm{X-}}^{\mathrm{T}} + \lambda\mathbf{I}\right)^{-1} \mathbf{M}_{\mathrm{X-}}\mathbf{T}_{\mathrm{X-}}^{\mathrm{T}} \tag{4}$$

$$\mathbf{w}_{\mathrm{Y+}} = \left(\mathbf{M}_{\mathrm{Y+}}\mathbf{M}_{\mathrm{Y+}}^{\mathrm{T}} + \lambda\mathbf{I}\right)^{-1} \mathbf{M}_{\mathrm{Y+}}\mathbf{T}_{\mathrm{Y+}}^{\mathrm{T}} \tag{5}$$

$$\mathbf{w}_{\mathrm{Y-}} = \left(\mathbf{M}_{\mathrm{Y-}}\mathbf{M}_{\mathrm{Y-}}^{\mathrm{T}} + \lambda\mathbf{I}\right)^{-1} \mathbf{M}_{\mathrm{Y-}}\mathbf{T}_{\mathrm{Y-}}^{\mathrm{T}} \tag{6}$$

E. Detection phase

The process of detection phase in the proposed method, shown in Fig. 2 (b), starts with passing of the features $\mathbf{M}[:,n']$, extracted at time n', in the models of the 1st stage. Here n' is the index of time during the detection phase. It results to the estimation of the first stage $\hat{X}_{S1}[n']$, and $\hat{Y}_{S1}[n']$ as:

$$\hat{\mathrm{X}}_{\mathrm{S1}}[n'] = \mathbf{w}_{\mathrm{X}}\mathbf{M}[:,n'] \text{ and } \hat{\mathrm{Y}}_{\mathrm{S1}}[n'] = \mathbf{w}_{\mathrm{Y}}\mathbf{M}[:,n'] \tag{7}$$

As shown in Fig. 2 (b), the estimates of the 1st stage are then forwarded to the 2nd stage which are used to select the models as shown in the flowchart of Fig. 3. In order to avoid discontinuities between two models for a given direction, the models can be averaged depending to a certain threshold μ around 0. In our case, μ is fixed to 0.2. This is how the estimates $\hat{X}_{S2}[n']$, and $\hat{Y}_{S2}[n']$ of the 2nd stage were obtained (see the inputs in Fig. 3).

III. Offline and Online Results

In order to observe the behavior of the proposed two-stage regression structure, two types of evaluation were conducted with a single healthy and experienced adult participant: an offline evaluation and an online evaluation. In both cases, the results of the 2 stages are compared based on a large number of trials in order to provide relevant observations. The 1st stage corresponds to a conventional detection method and the 2nd stage represents the contribution of this paper. The movements and the EMG sensor used in this study are presented in Section II.A. We chose to use an experienced subject in this paper to assess the feasibility and effectiveness of the proposed approach by reducing the potential bias caused by using a non-experienced participant to control the cursor.

A. Offline Evaluation

For the offline evaluation, 10 acquisition sequences composed of X and Y movements have been recorded, as shown in Fig. 1 and detailed in section II.A. As explained in Section II, the data from data acquisition were used to create the models of the proposed structure. In order to evaluate this structure, the acquisition sequences were divided into training and test datasets using cross-validation for several training rates. This learning rate corresponds to the percentage of training data used for the learning phase: if this rate is 10%, then 10% of the data were used for training the models and 90% for testing them. This makes it possible to observe the impact of number of data used to create the models on performance. Different criteria were considered and presented in Fig. 4. This figure presents means and standard deviations of a maximum number of 60 cross-validation possibilities.

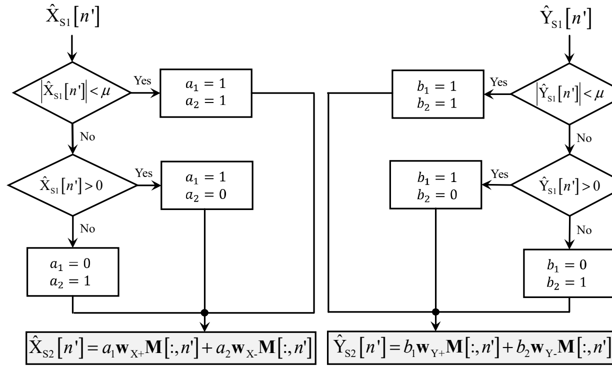

Figure 3. Flowchart for the selection and combination block of the 2nd stage (Fig. 2 (b)) in function of each direction to estimate the wrist DoFs.

The R-squared (R^2) and minimum mean square error (MMSE) criteria were used to evaluate the accuracy of the estimates with respect to the target data. The results of these criteria for the X and Y movements are shown in Fig. 4 (a, b, d, e) for both stages. All these results represent an improvement of the proposed structure (2nd stage) compared to the conventional regression approach (1st stage) in terms of accuracy (R^2 and MMSE) for X and Y movements of the wrist. Furthermore, in function of the learning rate, these results show the expected tendency: the more training data is used compared to the test data, the better performance we have. These results on accuracy (classically presented in this field) reveal the interest of the proposed structure, but the results of Fig. 4 (c) and Fig. 4 (f) especially show its potential.

The main goal of the proposed structure is to divide the DoFs into directions to improve the ability of the models to reach the target boundaries in each direction. In the present case, the two DoFs are divided in 4 directions. For this reason, the rate of reaching the boundaries was computed for both stages (see Fig. 4 (c)). This criterion simply shows that if the target is equal to a boundary, its estimate is also equal to the boundary value, for all directions. The average value of this rate is equal 79.9% (±6.7) for the 1st stage and equal to 97.1% (±2.1) for 2nd stage. These results mean that creating a model specifically for a given direction yields to achieve the boundaries imposed by the target in a relevant way.

One consequence of being better to reach the boundaries from the same input with the 2nd stage compared to the 1st stage is shown in Fig. 4 (f). In this figure, the average times between the time of reaching to the boundary for the 2nd stage and the time that the 1st stage manages to reach this boundary were presented. This difference of time is the advance time of

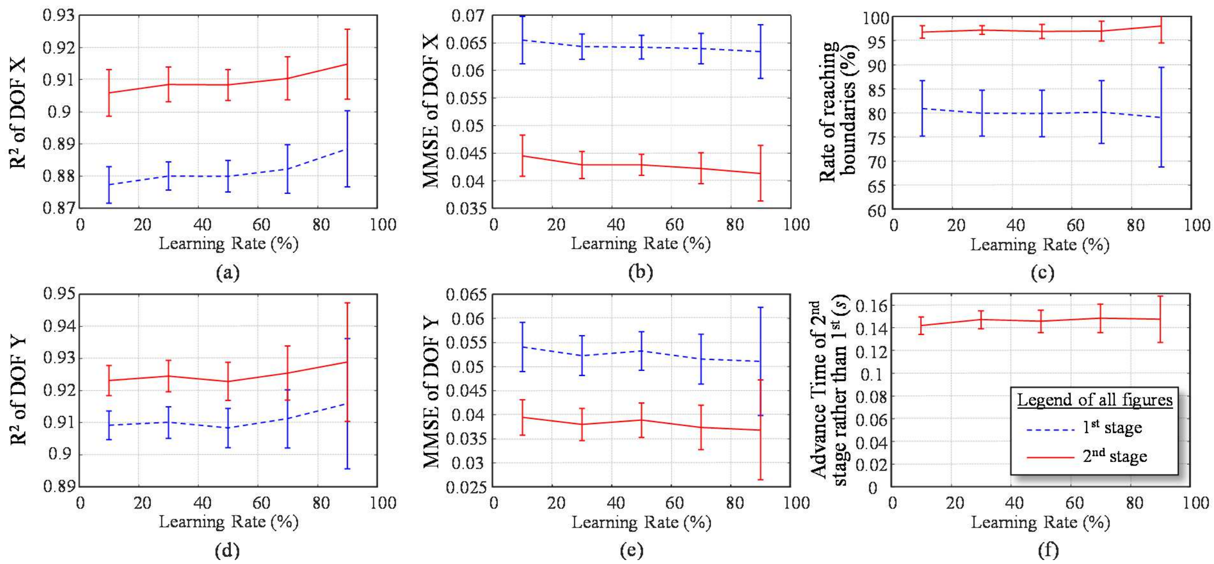

Figure 4. Results of the offline evaluation for the test data as a function of learning rate, for the 2 stages of the proposed detection structure, in terms of (a) R^2 for X, (d) R^2 for Y, (b) MMSE for X, (e) MMSE for Y, (c) rate of reaching boundaries and (f) advance time of the 2nd stage.

the 2nd stage compared to the 1st stage to reach the boundaries. For all learning rates, the average advance time is equal to 146 ms (±13). This means that the 2nd stage compared to the 1st stage allows for a more responsive movement estimation. Thus, the use of a 2nd stage of the proposed structure improves the overall performance in terms of accuracy, boundaries reaching and also reaction speed. The next section evaluates the usefulness of these improvements for simultaneous and proportional real-time control.

B. Online Evaluation

In order to evaluate the behavior of our simultaneous and proportional control structure based on EMG signals in real-time, the participant was asked to control a cursor on the screen with his wrist and to hit targets. All cursor trajectories obtained in this experiment and the 3 types of targets to be hit are presented in Fig. 5. The characteristics of these 3 targets are as follows: 3 different diameters as D_{diam}=[10, 25, 50] mm with the same distance of D_{dist}= 400 mm from the origin which are placed at 16 different angles separated by 22.5 degrees. Each target was appeared 4 times (4 trials) to the participant in a completely random way for each method. Each target appears subsequently, then the cursor is

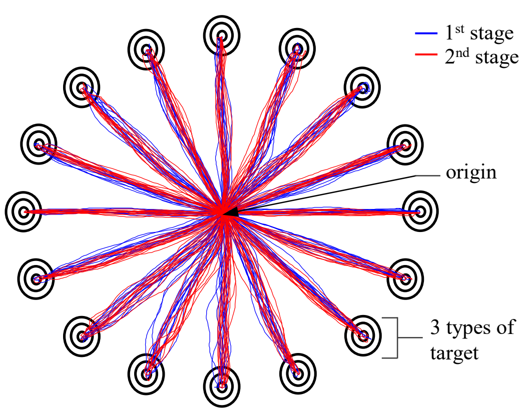

Figure 5. Cursor trajectories from the online control task obtained by the 2 stages of the proposed structure with the targets to be hit.

automatically returned to the origin for the next round by hitting the target. In addition, the subject had no idea whether he was controlling the cursor with the estimates from the 1st or 2nd stage of the structure. Note that the total trajectory of the cursor to its target is the sum of all X and Y displacements estimated at each sampling time by a given method. Finally, the structure models used here were built with the 10 acquisition sequences from the offline evaluation.

During the real-time task, several metrics were collected in order to calculate relevant evaluation criteria from Fitts' law [20]. First, the index of difficulty, *ID*, was calculated for each target by (8) which is a function of its diameter and its distance from the origin of the coordinate system.

$$ID = \log_2\left(\left(D_{dist}/D_{diam}\right)+1\right) \qquad (8)$$

Since the angle of the target rather than the origin does not appear in this equation and the distance to the origin is constant for all cases, only the diameter of the targets influences the value of *ID*. Thus, the *ID* values are equal to 3.2, 4.1 and 5.3 respectively for the target diameters of 50 mm, 25 mm and 10 mm. The higher this index is, the more difficult the task is. Then the data for each *ID* and each method were aggregated to calculate the two evaluation criteria in Fig. 6 which are path efficiency and completion time. Each mean and standard deviation values of Fig. 6 is obtained from 64 recorded data (4 trials × 16 angles).

The path efficiency, P_{eff}, Fig. 6 (a), is defined as a measure of the straightness of the cursor path to the target. The path efficiency is good for all methods and all *ID*s: the P_{eff} values are above 95%. It can be pointed out that, for the smallest target, the P_{eff} values are clearly affected and the 2nd stage returns a higher average P_{eff} compared to the 1st stage: 96.5% (±2.1) for the 1st stage and 97.3% (±1.4) for the 2nd stage. As can be seen in the offline evaluation, the contribution of the 2nd stage shows an interesting result in terms of accuracy, but this is not where its impact is most remarkable.

The completion times, T_c, which correspond to the time needed to hit a given target from the origin, are presented in

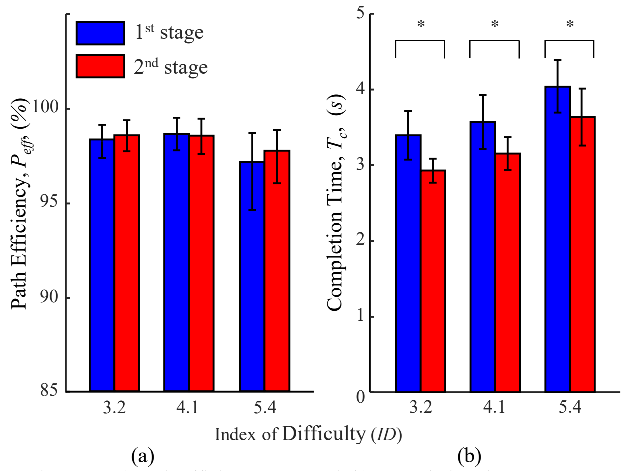

Figure 6. (a) Path efficiency, P_{eff}, and (b) Completion time, T_c, as a function of the index of difficulty (*ID*) from the online evaluation of the two stages.

Fig. 6 (b). For all methods, as the task becomes more difficult, the T_c is higher. For each *ID*, the time to complete the 2nd stage is significantly lower than the T_c of the 1st stage. A one-way ANOVA was performed on the T_c values of both stages for each *ID* and in each case the p-value was less than 0.005. For the three *ID*s, the average advance times of the 2nd stage relative to the 1st stage to hit the target are 466 ms, 421 ms and 406 ms respectively. According to the results in Fig. 6 (b), it is worth to mention that the time to hit the smallest target with the 2nd stage is close to the time to hit the 2 easiest targets with the 1st stage. The offline observations were confirmed when using the proposed method for real-time 2-DoF control to hit targets. The proposed two-stage regression structure improves the control accuracy while providing a more reactive control compared to the conventional regression approach.

IV. Conclusion

A two-stage regression structure was proposed to achieve a simultaneous and proportional control based on EMG signals. Instead of considering one regression model per DoF of the wrist, the proposed method allows the application of one regression model per wrist direction: the 1st stage based on DoF methods selects the direction models of the 2nd stage. Offline and online evaluations, performed in the 2-DoF case and with linear regression, have shown that the proposed structure improves the control accuracy while providing a significantly more reactive control compared to the conventional regression approach. The potential of this structure does not end here for the following three reasons which will be the subject of future works. Firstly, the linear regression methods considered can be replaced by other more efficient methods. Secondly, the proposed structure can be easily configured to detect 3 DoFs or more. Finally, a smart exploitation of the data from the 1st stage can be conducted to make a more relevant construction of the 2nd stage models. Future studies will involve several participants with no prior experience in EMG control to analyze the applicability and generalizability of the proposed method.

Acknowledgment

Research supported by Natural Sciences and Engineering Research Council of Canada (NSERC).

References

[1] L. Pan, D. L. Crouch, and H. Huang, "Comparing EMG-based human-machine interfaces for estimating continuous, coordinated movements," *IEEE transactions on neural systems and rehabilitation engineering,* vol. 27, no. 10, pp. 2145-2154, 2019.

[2] D. Yang, Y. Gu, N. V. Thakor, and H. Liu, "Improving the functionality, robustness, and adaptability of myoelectric control for dexterous motion restoration," *Experimental brain research,* vol. 237, pp. 291-311, 2019.

[3] F. Nougarou, A. Campeau-Lecours, D. Massicotte, M. Boukadoum, C. Gosselin, and B. Gosselin, "Pattern recognition based on HD-sEMG spatial features extraction for an efficient proportional control of a robotic arm," *Biomedical Signal Processing and Control,* vol. 53, p. 101550, 2019.

[4] P. Geethanjali, "Myoelectric control of prosthetic hands: state-of-the-art review," *Medical Devices (Auckland, NZ),* vol. 9, p. 247, 2016.

[5] C. Chen, Y. Yu, X. Sheng, D. Farina, and X. Zhu, "Simultaneous and proportional control of wrist and hand movements by decoding motor unit discharges in real time," *Journal of Neural Engineering,* vol. 18, no. 5, p. 056010, 2021.

[6] W. Yang, D. Yang, Y. Liu, and H. Liu, "Decoding simultaneous multi-DOF wrist movements from raw EMG signals using a convolutional neural network," *IEEE Transactions on Human-Machine Systems,* vol. 49, no. 5, pp. 411-420, 2019.

[7] Q. Zhang, T. Pi, R. Liu, and C. Xiong, "Simultaneous and proportional estimation of multijoint kinematics from EMG signals for Myocontrol of robotic hands," *IEEE/ASME Transactions on Mechatronics,* vol. 25, no. 4, pp. 1953-1960, 2020.

[8] M. Nowak, I. Vujaklija, A. Sturma, C. Castellini, and D. Farina, "Simultaneous and Proportional Real-Time Myocontrol of up to three Degrees of Freedom of the Wrist and Hand," *IEEE Transactions on Biomedical Engineering,* 2022.

[9] J. M. Hahne, M. A. Wilke, M. Koppe, D. Farina, and A. F. Schilling, "Longitudinal case study of regression-based hand prosthesis control in daily life," *Frontiers in neuroscience,* vol. 14, p. 600, 2020.

[10] S. Abbaspour, A. Naber, M. Ortiz-Catalan, H. GholamHosseini, and M. Lindén, "Real-time and offline evaluation of myoelectric pattern recognition for the decoding of hand movements," *Sensors,* vol. 21, no. 16, p. 5677, 2021.

[11] K. H. Lee, J. Y. Min, and S. Byun, "Electromyogram-based classification of hand and finger gestures using artificial neural networks," *Sensors,* vol. 22, no. 1, p. 225, 2021.

[12] J. Luo, C. Liu, and C. Yang, "Estimation of EMG-based force using a neural-network-based approach," *IEEE Access,* vol. 7, pp. 64856-64865, 2019.

[13] Z. Zhang, K. Yang, J. Qian, and L. Zhang, "Real-time surface EMG pattern recognition for hand gestures based on an artificial neural network," *Sensors,* vol. 19, no. 14, p. 3170, 2019.

[14] T. Bao, S. A. R. Zaidi, S. Xie, P. Yang, and Z.-Q. Zhang, "A CNN-LSTM hybrid model for wrist kinematics estimation using surface electromyography," *IEEE Transactions on Instrumentation and Measurement,* vol. 70, pp. 1-9, 2020.

[15] X. Chen, Y. Li, R. Hu, X. Zhang, and X. Chen, "Hand gesture recognition based on surface electromyography using convolutional neural network with transfer learning method," *IEEE Journal of Biomedical and Health Informatics,* vol. 25, no. 4, pp. 1292-1304, 2020.

[16] Y. Wen, S. Avrillon, J. C. Hernandez-Pavon, S. J. Kim, F. Hug, and J. L. Pons, "A convolutional neural network to identify motor units from high-density surface electromyography signals in real time," *Journal of neural engineering,* vol. 18, no. 5, p. 056003, 2021.

[17] A. Fougner, Ø. Stavdahl, P. J. Kyberd, Y. G. Losier, and P. A. Parker, "Control of upper limb prostheses: Terminology and proportional myoelectric control—A review," *IEEE Transactions on neural systems and rehabilitation eng.,* vol. 20, no. 5, pp. 663-677, 2012.

[18] I. Vujaklija, V. Shalchyan, E. N. Kamavuako, N. Jiang, H. R. Marateb, and D. Farina, "Online mapping of EMG signals into kinematics by autoencoding," *Journal of neuroengineering and rehabilitation,* vol. 15, no. 1, pp. 1-9, 2018.

[19] C. Spiewak, M. Islam, A. Zaman, and M. H. Rahman, "A comprehensive study on EMG feature extraction and classifiers," *Open Access Journal of Biomedical Engineering and Biosciences,* vol. 1, no. 1, pp. 1-10, 2018.

[20] A. Ameri, M. A. Akhaee, E. Scheme, and K. Englehart, "Regression convolutional neural network for improved simultaneous EMG control," *Journal of neural engineering,* vol. 16, no. 3, p. 036015, 2019.